Astrophysical S-factor of the ³He(α,γ)⁷Be reaction measured at low energy via prompt and delayed γ detection

F. Confortola,[1] D. Bemmerer,[2, *] H. Costantini,[1] A. Formicola,[3] Gy. Gyürky,[4] P. Bezzon,[5] R. Bonetti,[6] C. Broggini,[2, †] P. Corvisiero,[1] Z. Elekes,[4] Zs. Fülöp,[4] G. Gervino,[7] A. Guglielmetti,[6] C. Gustavino,[3] G. Imbriani,[8] M. Junker,[3] M. Laubenstein,[3] A. Lemut,[1] B. Limata,[9] V. Lozza,[2] M. Marta,[6] R. Menegazzo,[2] P. Prati,[1] V. Roca,[9] C. Rolfs,[10] C. Rossi Alvarez,[2] E. Somorjai,[4] O. Straniero,[8] F. Strieder,[10] F. Terrasi,[11] and H.P. Trautvetter[10]

(The LUNA Collaboration)

[1]Università degli Studi Genova & INFN Genova, Via Dodecaneso 33, 16146 Genova, Italy
[2]INFN Sezione di Padova, Via Marzolo 8, 35131 Padova, Italy
[3]INFN, Laboratori Nazionali del Gran Sasso, S.S. 17bis km 18.890, Assergi, L'Aquila, Italy
[4]ATOMKI, Debrecen, Hungary
[5]INFN, Laboratori Nazionali di Legnaro, Padova, Italy
[6]Istituto di Fisica Generale Applicata, Università di Milano & INFN Milano, Milano, Italy
[7]Dipartimento di Fisica Sperimentale, Università di Torino & INFN Torino, Torino, Italy
[8]INAF, Osservatorio Astronomico di Collurania, Teramo, Italy
[9]Dipartimento di Scienze Fisiche, Università "Federico II" & INFN Napoli, Napoli, Italy
[10]Institut für Experimentalphysik III, Ruhr-Universität Bochum, Bochum, Germany
[11]Dipartimento di Scienze Ambientali, Seconda Università di Napoli, Caserta & INFN Napoli, Napoli, Italy
(Dated: February 1, 2008)

Solar neutrino fluxes depend both on astrophysical and on nuclear physics inputs, namely on the cross sections of the reactions responsible for neutrino production inside the Solar core. While the flux of solar ⁸B neutrinos has been recently measured at Superkamiokande with a 3.5% uncertainty and a precise measurement of ⁷Be neutrino flux is foreseen in the next future, the predicted fluxes are still affected by larger errors. The largest nuclear physics uncertainty to determine the fluxes of ⁸B and ⁷Be neutrinos comes from the ³He(α,γ)⁷Be reaction. The uncertainty on its S-factor is due to an average discrepancy in results obtained using two different experimental approaches: the detection of the delayed γ rays from ⁷Be decay and the measurement of the prompt γ emission. Here we report on a new high precision experiment performed with both techniques at the same time. Thanks to the low background conditions of the Gran Sasso LUNA accelerator facility, the cross section has been measured at E_{cm} = 170, 106 and 93 keV, the latter being the lowest interaction energy ever reached. The S-factors from the two methods do not show any discrepancy within the experimental errors. An extrapolated S(0)= 0.560±0.017 keV barn is obtained. Moreover, branching ratios between the two prompt γ-transitions have been measured with 5-8% accuracy.

Forty years ago, John Bahcall and Raymond Davis started to explore the solar interior by studying the neutrinos emitted by the Sun [1]. The results of the first neutrino detection experiment [2] originated the so called solar neutrino puzzle, consisting in a deficit of measured neutrinos with respect to the theoretical predictions of the Standard Solar Model (SSM). After thirty years of experiments, SNO and Kamland [3, 4] observed neutrino oscillations and proved that the missing solar electron neutrinos actually change their flavour during the travel to the Earth. This closed the neutrino puzzle. Therefore, the high precision measurement of ⁸B neutrino flux [5], together with the foreseen measurement of ⁷Be neutrinos [6], can now be used to understand physical and chemical properties of the Sun, provided that nuclear re-

action cross sections are known with similar accuracy [7]. The ³He(α,γ)⁷Be reaction is the onset of the ⁷Be and ⁸B branches of the proton-proton (p-p) chain of hydrogen burning. The 9% error [8] on its cross section is presently the main nuclear physics uncertainty on the prediction of ⁷Be and ⁸B neutrino fluxes [9].

At stellar energies the ³He(α,γ)⁷Be cross section σ(E) drops exponentially with the energy and can be parametrized as:

$$\sigma(E) = \frac{S(E)}{E} e^{-2\pi\eta(E)} \tag{1}$$

where S(E) is the astrophysical factor, η is the Sommerfeld parameter [10], and E is the center of mass energy.

³He(α,γ)⁷Be is a radiative capture reaction (Q-value: 1.586 MeV) into the first excited state (E_x=429 keV) and the ground state of ⁷Be that subsequently decays by electron capture into ⁷Li with a terrestrial half life of 53.22±0.06 days [11].

In the last forty years the ³He(α,γ)⁷Be reaction has been measured using two techniques. In the first ap-

---

proach direct α-capture γ-rays were detected (prompt γ method) [12, 13, 14, 15, 16, 17, 18], while, in the second, the delayed ^{7}Be-decay γ rays were counted (activation method) [12, 19, 20, 21]. Previous activation results are, on the average, 13% higher than prompt γ data and this is the origin of the large uncertainty quoted on the reaction cross section [8]. Up to now, no explanation has been obtained for this discrepancy that could be due either to systematic experimental errors (angular distribution, branching ratio effects, parasitic reactions producing ^{7}Be) or to the existence of a non radiative capture (E0 monopole) [22]. Recently, the discrepancy on the extrapolated S(0) has been reduced by an activation study at 420<E<950 keV [21] to 9%. High accuracy (4%) activation data were obtained also at LUNA, at center of mass energies down to 106 keV [23, 24]. Nevertheless, high accuracy prompt gamma data are also needed to verify the claimed discrepancy.

We have performed a new high accuracy measurement using simultaneously prompt and activation methods with the same experimental setup. The experiment has been carried out using the underground LUNA 400 kV accelerator [25] at the Gran Sasso National Laboratory (LNGS).

Three couples of cross section values have been measured (prompt γ and activation) at E_α=220, 250 and 400 keV. A sketch of the interaction chamber is given in Fig. 1. The α beam enters the ^{3}He extended windowless gas target [24] through a 7 mm diameter collimator and is stopped on a detachable copper disk that serves as the primary catcher for the produced ^{7}Be and as the hot side of a calorimeter [26]. The latter measures the beam intensity (about 250 μA) with an accuracy of 1.5%. The high beam current decreases the ^{3}He density along the beam path [27]: this effect has been monitored with a silicon detector by double Rutherford scattering providing an accuracy of 1.3% on the gas density determination [28]. The same detector is also used to measure the gas contamination (mainly N_2) that has remained below (2.7 $\pm$ 0.3)%.

Prompt γ rays are counted with a 135% ultra low-background HPGe detector shielded with 5 cm of OFHC copper and 25 cm of lead. The detector and the shield are enclosed in a sealed plastic box flushed with dry N_2 to reduce ^{222}Rn background. Thanks to the underground environment where cosmic muons are strongly reduced [29], the shielding suppression factor is of five orders of magnitude for γ rays below 2 MeV. A lead collimator is positioned inside the target chamber to collect mostly γ rays emitted at 55°. At this angle the contribution of the second Legendre polynomial in the angular distribution expression, vanishes. Therefore the inner collimator reduces the systematic error due to prompt γ angular distribution uncertainties and also shields the detector from possible beam-induced radiation coming from the entrance collimator and the calorimeter cap. The effective target length seen by the HPGe detector is approximately 12 cm, corresponding to an energy loss $\Delta E = 3$
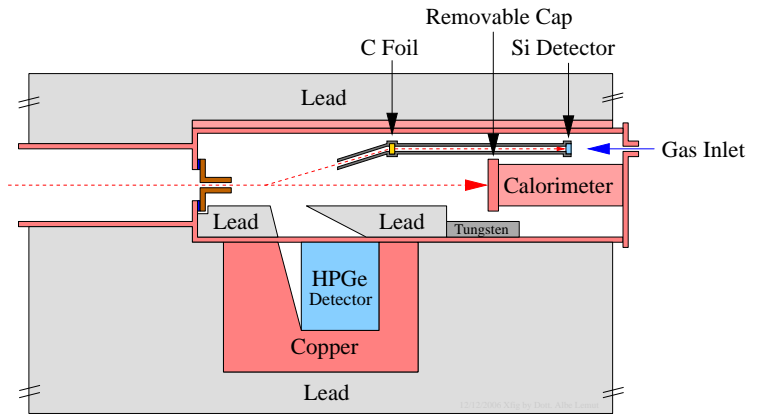

FIG. 1: Schematic view of the interaction chamber with the position of the HPGe detector and of the 100 μm silicon detector used for ^{3}He density monitoring. The distance between the entrance collimator and the calorimeter is 35 cm. The thickness of the internal collimator is 3 cm for the Lead part and 1.6 cm for the Tungsten part.

keV at P_{target}=0.7 mbar (value used in all the runs) and E_α=400 keV.

The photopeak detection efficiency is determined by a Monte Carlo code [30] calibrated with ^{60}Co and ^{137}Cs radioactive point-like sources moved along the beam path. The Monte Carlo reproduces the experimental efficiency within the source activity uncertainties (1.5%). The spectra collected at E_α= 220, 250 and 400 keV, with a total charge of 637, 407 and 113 C respectively, are shown in Fig. 2 together with laboratory background. Beam induced gamma-ray background has been measured with ^{4}He gas in the target at E_α= 400 keV: no difference with laboratory background has been observed. In the data analysis only the two primary transitions at E_γ=Q+E_{cm} and E_γ=Q+E_{cm}−429 keV, have been considered. Theoretical angular distribution functions are calculated by [31] down to 210 keV interaction energy. A linear extrapolation of the curves of [31] has been done and the coefficients of the Legendre polynomials adopted in the detection efficiency calculation are: a_1= - 0.05 and a_1 = 0 for the transition to the ground and to the first excited state, respectively and a_2= - 0.1 for both transitions. These values are in agreement with recent theoretical predictions [32]. With the Monte Carlo code, we have conservatively varied 100% both a_1 and a_2 coefficients obtaining a global 2.5% variation of the detection efficiency. This value has been assumed as a systematic uncertainty and turns out to be the major contribution to the error budget of the prompt γ method. The in-beam runs provide accurate branching ratios between the two transitions σ(DC$\to$ 429)/σ(DC$\to$0): 0.417 ±0.020, 0.415±0.029 and 0.38±0.03 at E_α = 400, 250 and 220 keV, respectively. Our values are consistent with, but more precise than, latest branching ratio measurements [12, 16] and are in agreement with theoretical calculations [33].
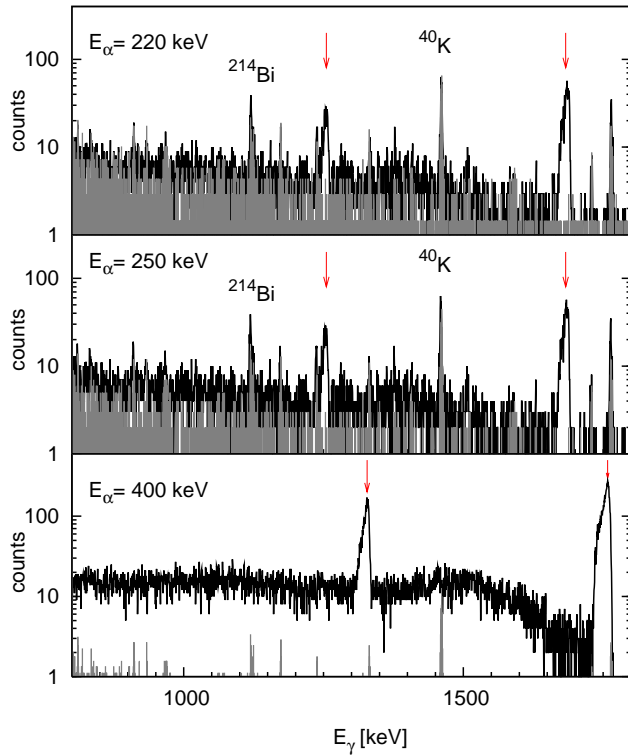
FIG. 2: γ-ray spectrum at $E_\alpha = 220$, 250 and 400 keV compared with natural laboratory background (in grey) normalized to beam-measurement live times (respectively: 31.2 days, 21.3 days and 4.8 days). Arrows indicate the primary transition peaks to the first excited state and to the ground state.

During the runs in which prompt γ-rays are detected, the ^{7}Be nuclei produced inside the gas target get implanted into the removable calorimeter cap. After each run, the cap is dismounted and moved to LNGS underground low-activity counting facility [29]. Details and accuracy of the activation method at LUNA are discussed elsewhere [23, 24]. Since we have simultaneously used the same beam and target for both methods, some systematic uncertainties (beam intensity, target density and purity) cancel out in the comparison between the two techniques.

Results are reported in Table I and shown in Fig. 3 together with all previous literature data. For each couple of data (prompt γ and activation) obtained at the same E_α, the effective energy (E_{eff}), calculated as described in [23], is slightly different. Indeed the target of the prompt γ experiment, defined by the inner collimator (Fig. 1), is a fraction of the whole target contributing to ^{7}Be production. The E_{eff} difference corresponds to an S-factor change smaller than 0.1% according to the

energy dependence given in [34]. In the comparison between prompt and activation S-factors, we have therefore neglected the E_{eff} differences and considered a total uncertainty given by the statistical and reduced systematic errors summed in quadrature (Table I). The mean percentage difference between the S-factor values in Table I ($\Delta S=(S_a-S_p)/((S_a+S_p)/2)$) is $\Delta S_m = -0.014\pm0.042$. This result limits to $+2.8\%$ (maximum ΔS_m value at 1σ level) possible non-radiative contributions to the reaction cross section. S-factor activation values at $E_\alpha=400$ and 250 keV are compatible with those previously obtained at LUNA with the same setup [23, 24]. Considering the average of the new and old activation values at the same beam energy, ΔS_m does not change. A simultaneous measurement with both activation and prompt γ technique at energies around $E_{cm}=1$ MeV, where the oldest activation experiments [12, 19] were performed, would be useful to look for non-radiative contributions in a higher energy region than the one explored in the present experiment. To deduce the extrapolated S(0), the fit of [34] has been rescaled using the present activation and prompt γ data separately. The weighted average between the two S(0) values has been calculated adopting as weights the statistical error obtained from the fit and the reduced systematic error. We get S(0)=0.560±0.017 keV barn where the final uncertainty also includes the systematic error common to the two methods. Performing the same calculation considering also the most recent and very accurate results from [21, 23, 24] or using the theoretical function [35] adopted in the NACRE compilation [36], instead of the R-matrix fit by [34], the extrapolated S(0) changes less than 1%. Low energy accurate data in fact minimize the uncertainty upon extrapolation. However, a refined measurement of the slope of the S-factor in a wide energy range would be useful to confirm theoretical calculations reducing the uncertainty on the extrapolated S(0). The uncertainty on the predicted ^{8}B neutrino flux due to S_{34} is now reduced from 7.5% to 2.4% and the total uncertainty, including astrophysical parameters, goes from 12% to 10% [37]. Similarly, the uncertainty on ^{7}Be predicted flux goes from 9.4% to 5.5%, being the contribution of S_{34} error reduced from 8% to 2.5% [37].

[1] J. N. Bahcall, Phys. Rev. Lett. **12**, 300 (1964).
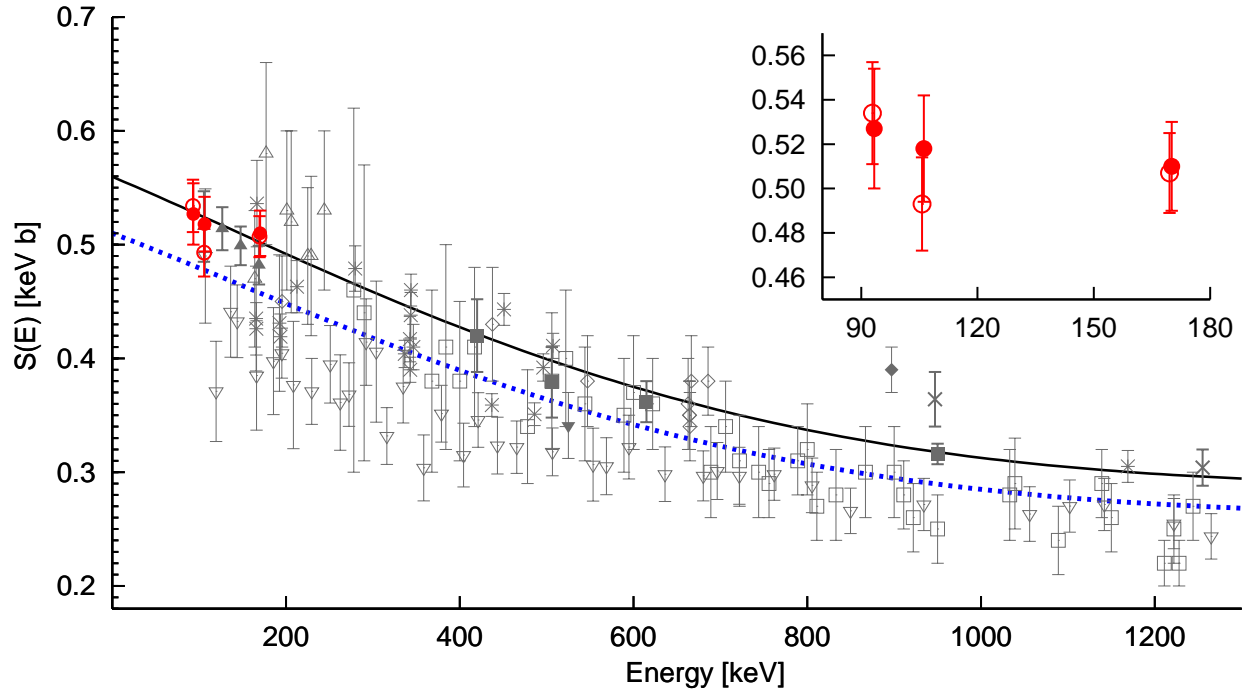
[2] R. Davis, Phys. Rev. Lett. **12**, 303 (1964).

FIG. 3: Overview of all available S-factor values for the $^3\mathrm{He}(\alpha,\gamma)^7\mathrm{Be}$ reaction. Filled and open circles: present work. Prompt-γ data: open squares [14], open triangles [15], stars [12], open inverse triangles [16], filled inverse triangles [17], open diamonds [18]. Activation data: filled diamonds [19], crosses [12], filled squares [21], filled triangles [23, 24]. Dashed line: most recent R-matrix fit [34], solid line: fit [34] normalized to present data. In the inset a zoom of prompt γ (filled circles) and activation (open circles) data obtained in this work.

[3] Q. R. Ahmad *et al.*, Phys. Rev. Lett. **87**, 71301 (2001).
[4] K. Eguchi *et al.*, Phys. Rev. Lett. **90**, 21802 (2003).
[5] J. Hosaka *et al.*, Phys. Rev. D **73**, 112001 (2003).
[6] G. Alimonti *et al.*, Astropart. Ph. **16**, 205 (2002).
[7] G. Fiorentini and B. Ricci, astro-ph/0310753 (2003).
[8] E. Adelberger *et al.*, Rev. Mod. Phys. **70**, 1265 (1998).
[9] J. N. Bahcall and M. H. Pinsonneault, Phys. Rev. Lett. **92**, 121301 (2004).
[10] C. Rolfs and W. S. Rodney, *Cauldrons in the Cosmos* (University of Chicago Press, 1988).
[11] D. Tilley *et al.*, Nuc. Phys. A **708**, 3 (2002).
[12] J. Osborne *et al.*, Phys. Rev. Lett. **48**, 1664 (1982).
[13] H. Holmgren and R. Johnston, Phys. Rev. **113**, 1556 (1959).
[14] P. Parker and R. Kavanagh, Phys. Rev. **131**, 2578 (1963).
[15] K. Nagatani, M. R. Dwarakanath, and D. Ashery, Nucl. Phys. A **128**, 325 (1969).
[16] H. Kräwinkel *et al.*, Z. Phys. A **304**, 307 (1982).
[17] T. Alexander *et al.*, Nucl. Phys. A **427**, 526 (1984).
[18] M. Hilgemeier *et al.*, Z. Phys. A **329**, 243 (1988).
[19] R. Robertson *et al.*, Phys. Rev. C **27**, 11 (1983).
[20] H. Volk *et al.*, Z. Phys. A **310**, 91 (1988).
[21] B. N. Singh *et al.*, Phys. Rev. Lett. **93**, 262503 (2004).
[22] M. Nessin, T. H. Kruse, and K. E. Eklund, Phys. Rev. **125**, 639 (1962).

[23] D. Bemmerer *et al.*, Phys. Rev. Lett. **97**, 122502 (2006).
[24] G. Gyürky *et al.*, Phys. Rev. C **75**, 35805 (2007).
[25] A. Formicola *et al.*, Nucl. Instr. Meth. Phys. Res. A **507**, 609 (2003).
[26] C. Casella *et al.*, Nucl. Instr. Meth. Phys. Res. A **489**, 160 (2002).
[27] J. Görres *et al.*, Nucl. Instr. Meth. Phys. Res. **177**, 295 (1980).
[28] M. Marta *et al.*, Nucl. Instr. Meth. Phys. Res. A **569**, 727 (2006).
[29] C. Arpesella *et al.*, Appl. Radiat. Isot. **47**, 991 (1996).
[30] C. Arpesella *et al.*, Nucl. Instr. Meth. Phys. Res. A **360**, 607 (1995).
[31] T. A. Tombrello and P. D. Parker, Phys. Rev. **131**, 2582 (1963).
[32] B. T. Kim, T. Izumoto, and K. Nagatani, Phys. Rev. C **23**, 33 (1981).
[33] T. Kajino, Nucl. Phys. A **460**, 559 (1986).
[34] P. Descouvemont *et al.*, At. Data and Nuc. Data. Tab. A **88**, 203 (2004).
[35] T. Kajino H. Toki and S. M. Austin, Astrophys. J. **319**, 531 (1987).
[36] C. Angulo *et al.*, Nucl. Phys. A **656**, 3 (1999).
[37] C. Peña Garay, private comunication (2006).

Eα (keV)	Method	E$_{eff}$ (keV)	σ(E$_{eff}$) (nbarn)	S(E$_{eff}$) (keV barn)	ΔS stat. (keV barn)	ΔS syst. (keV barn)	ΔS red. syst. (keV barn)
400	p	170.1	10.25	0.510	0.008	0.019	0.015
400	a	169.5	10.00	0.507	0.010	0.015	0.010
250	p	106.1	0.588	0.518	0.014	0.019	0.016
250	a	105.7	0.546	0.493	0.015	0.015	0.011
220	p	93.3	0.235	0.527	0.018	0.020	0.016
220	a	92.9	0.232	0.534	0.016	0.017	0.013

TABLE I: Cross section and S-factor results with corresponding uncertainties for the prompt (p) and activation (a) methods. In the last column the reduced systematic uncertainty is reported where contributions common to the two methods have been subtracted.